Electrochemical Characterization of the Oxidation of LB Films of Polyphthalocyaninatosiloxane

A. Ferencz,† N. R. Armstrong,*,†,‡ and G. Wegner*,†

Max Planck Institut für Polymerforschung, Ackermannweg 10, D-6500 Mainz, Germany, and Department of Chemistry, University of Arizona, Tucson, Arizona 85721

Received October 25, 1993•

ABSTRACT: Highly ordered PcPS (phthalocyaninatopolysiloxane) thin films have been produced on a variety of substrates using Langmuir–Blodgett thin-film deposition techniques, with coverages ranging from 1 to 100 molecular layers. Siloxane-polymerized cofacial phthalocyanines, with alkoxyhydrocarbon side chains on the individual Pc units, yield molecules capable of forming highly ordered, densely packed LB films, with individual polymeric-Pc chains ranging in size up to ca. 100 Pc monomer units each. These ultrathin films shows facile electron and ion transport during electrochemical and chemical oxidation and notable stability of the Pc cation radicals in the polymer chains in contact with *both* aqueous and nonaqueous media. Coulometric and spectroelectrochemical data suggest the oxidation of at least 80 → 100% of the Pc rings at potentials up to ca. 1.0 V and the onset of formation of Pc dication species. There is a strong anion dependence for both the extent and rate of oxidation of the PcPS films in aqueous media. Anion incorporation can occur over a wide potential range from aqueous media, however, without the apparent loss of film structure or stability.

Introduction

Ultrathin polymer films comprised of redox active molecules have a considerable history of investigation.[1-9] Easily processable forms of these polymers are especially interesting if, when appropriately "doped", they take on high electronic or ionic conductivities. Electrodes modified with highly ordered redox systems such as self-assembled (SA) monolayers, or systems depositable as Langmuir–Blodgett thin films, are now receiving more attention.[10]

Cofacial, siloxane-polymerized phthalocyanines (phthalocyaninatopolysiloxanes, PcPS), with individual phthalocyanine rings spaced at ca. 3.3 Å, have been made with alkoxyhydrocarbon side chains on the individual Pc units.[5,6] These "hairy-rod" polymers are capable of forming highly ordered Langmuir–Blodgett films on a variety of substrates, with coverages ranging from 1 to 100 molecular layers. (A schematic for the PcPS molecules of this study is shown in Figure 1, with the alkoxy substituents R_1 = OCH_3, R_2 = OC_8H_{17}.) Individual polymeric PcPS units range in size up to ca. 100 Pc monomer units each and form densly packed, strongly dichroic films. The linear/nonlinear optical properties and chemical sensor possibilities of PcPS thin films have been previously characterized.[6b,e,f] The addition of polymerizable groups in the side chains of PcPS (e.g., a double bond in the last hydrocarbon position of the alkoxy substituent, R_2 = C_8H_{15}) also adds the possibility for lithographic processing of these thin films into ultrasmall structures,[6i] which may be independently addressable by electrochemical means. The exploitation of PcPS and related materials as electrochemically "addressable" molecular arrays, and as the active interface in chemical sensors, requires a better understanding of thin-film structure and chemistry with regard to the transport of both electrical and ionic charge through the LB–PcPS thin film.

Cofacially polymerized unsubstituted, crystalline silicon phthalocyanines predate the PcPS system and have been of interest because of the wide range of dark conductivities

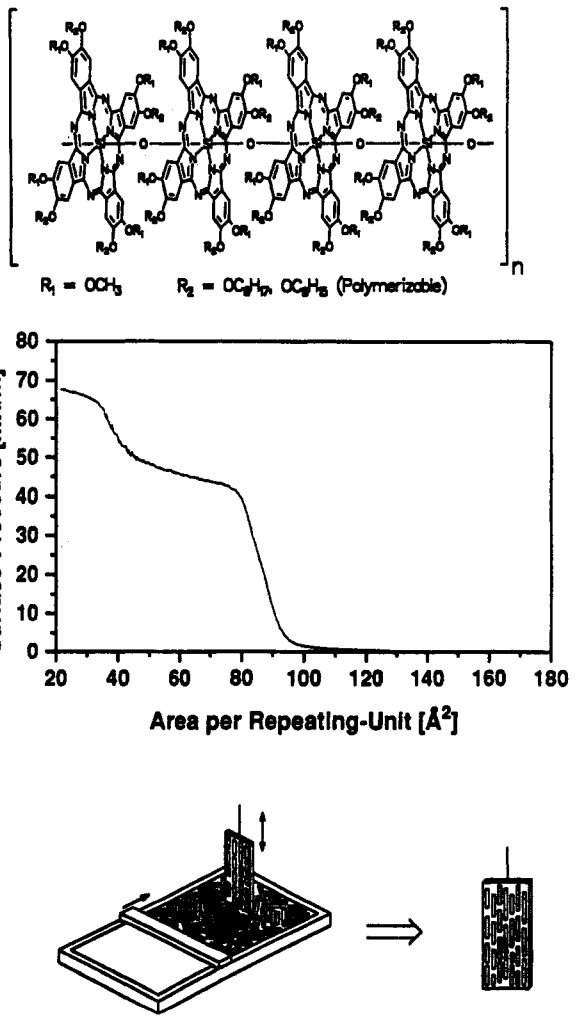

Figure 1. Schematic view of PcPS, a typical surface pressure/area per molecule diagram, and a schematic view of the organization of these rodlike polymers during the LB film formation process. The spacing between SiPc rings is ca. 3.3 Å, and the number of Pc units per PcPS rod can be as high as 50–100.

achievable as the doping level is varied.[11] Recent electrochemical doping studies of the crystalline powders of

* To whom correspondence should be addressed.
† Max Planck Institut für Polymerforschung.
‡ University of Arizona.
• Abstract published in *Advance ACS Abstracts*, February 1, 1994.

0024-9297/94/2227-1517$04.50/0

polymerized SiPc show that, at high overpotentials and electrolysis times of days, the extent of oxidative doping and the counterion-to-Pc ratio (X/Pc) can be increased to near 0.7.[11a,b] The high overpotentials associated with these doping processes were due in part to the difficulty of efficient oxidation of crystalline insoluble powders. In a more recent report, Gaudiello and Gale studied the electrochemical oxidation of polymerized versions of SiPc's, which had been previously modified with *tert*-butyl groups at the four benzenoid rings to improve solubility and to allow for direct electrochemical characterization of the SiPc polymer in tetrachloroethane.[11f] This improvement in solubility appeared to lower the overpotential for oxidation of the SiPc rings and gave electrochemical responses with some similarities to the data reported below, and some significant differences which will be discussed.

We report here on the first steps of electrochemical and spectroelectrochemical characterization of LB films of PcPS, interfaced to thin film gold, indium–tin oxide (ITO), and platinum electrodes, in contact with nonaqueous and aqueous electrolytes. These ultrathin LB films show facile electron and ion transport during oxidation of 80 → 100% of the Pc rings per PcPS unit and notable stability of the Pc cation radicals formed during oxidation in *both* aqueous and nonaqueous media. Counterion transport appears to control both the extent and rate for oxidation of the PcPS films in aqueous media but occurs without the loss of long-range film structure or stability.

Experimental Section

The synthesis and characterization of LB film-forming PcPS has been described in detail elsewhere.[6] The dichlorosilicon phthalocyanine monomer was first created with appropriate length hydrocarbon side chains, as shown schematically in Figure 1. The highest molecular weight (HMW) PcPS currently available (used for these studies) was obtained by initiation of the polymerization process in pyridine to give a soluble, low molecular weight oligomer, which was then isolated. Spectroscopic and gel permeation chromatographic (GPC) analysis of the oligomeric PcPS showed that it consisted primarily of the dimer SiPc fragment, with lower concentrations of monomer, trimer, and tetramer. This oligomer mixture was then allowed to polymerize further in diglyme for reaction times (up to 48 h) until the final high molecular weight product was achieved. Polymerization was allowed to proceed for lengths of time capable of forming cofacially polymerized Pc units with an average of 50–100 monomer units per polymer molecule. Different reaction times appeared to form different average length polymers and had a significant effect on both the visible spectroscopy and the electrochemistry of the resultant LB films (see below). The high molecular weight product was then washed repeatedly in methanol/chloroform mixed solvents and membrane filtered before use in LB film formation. The low molecular weight oligomer has also shown itself to be capable of forming LB layers, and the characterization of such thin films is also shown below for comparison with the electrochemical behavior of the high molecular weight PcPS films.

The soluble polymeric material was transferred to the LB trough with protocols already described.[6] Well-defined pressure–area isotherms were observed (Figure 1). Transfer typically occurred at pressures of 25 mN/m^2. Transfer ratios, unless otherwise stated, were between 0.9 and 1.0 for all layers deposited, on all substrates, and for all layer thicknesses. X-ray and electron diffraction studies of annealed and unannealed versions of these films have been carried out (6 h), and have shown that properly annealed PcPS films produce molecular columns which pack in hexagonal arrays, with the polymer chains parallel to the surface, demonstrating considerable long-range order, column diameters of 20–22 Å, and projected areas per Pc unit (within each PcPS molecule) of 85 Å.^{2}

The electrode substrates used in these studies were of three types. Gold optically transparent electrodes were ca. 300 Å of Au on polycarbonate substrates or polyethyleneterphthalate, whose electrochemical properties have been characterized before.[14] These electrodes present an exceptionally smooth substrate to the PcPS films, especially versus the ITO electrodes discussed below, showing defect sizes on average less than 250 Å in diameter over large regions of the Au-coated surface. These electrodes were cleaned by immersion in ethanol for 15 min during ultrasonic cleaning and were then immersed directly in the LB trough without further pretreatment. These Au electrodes had a sufficiently hydrophilic surface that optimal LB film formation was achieved by immersing the electrode in the aqueous subphase first, filling the LB trough with the appropriate amount of PcPS in chloroform, and then emmersing the Au surface to pick up the first PcPS monolayer. Normal sputtered or evaporated Au thin-film surfaces used in previous studies acquired a sufficiently hydrophobic character after exposure to ambient laboratory conditions that they could be immersed directly for acquisition of the first PcPS layer.[6] Pt electrodes, created by a sputtering process to give the optically transparent electrode on a glass or quartz substrates, were pretreated by plasma cleaning (Ar, 0.9 mbar, O_2, 0.1 mbar, 400 W) and were immersed immediately in the PcPS-coated LB trough, achieving a hydrophobic surface character immediately upon removal from the plasma cleaner. Indium tin oxide electrodes were of two forms and had sheet resistances of ca. 15 Ω and 100 Ω per square and an absorptivity across the visible wavelength region of less than 0.1. These electrodes were cleaned ultrasonically in ethanol/chloroform, plasma cleaned at 400 W, as for the Pt electrodes, immersed in 0.1 N HNO_3 for 10 min, immediately immersed in a neat solution of hexamethyldisilazane (HMDS) for 60 min, washed with 2-propanol, and then inserted directly in the PcPS-coated LB trough.

Unless otherwise stated, the cell used in this study was a simple variation on cells used for many of our past photoelectrochemical and spectroelectrochemical studies.[14,15a–c] The optically transparent electrodes were sandwiched against the electrolyte solution with a defined electrode area of 0.7 cm^2. The reference electrode was a silver wire, freshly anodized in saturated KCl, and placed in contact with a 0.1 M HNO_3 solution, isolated from the electrolyte by a Vycor glass frit. This reference electrode was calibrated against a true Ag/AgCl reference electrode, and the different electrolytes and potentials are thus reported against the Ag/AgCl reference couple. In CH_3CN experiments the reference electrode was a silver wire, freshly anodized in a 0.1 M $LiClO_4$ solution in CH_3CN. At the completion of each of the experiments in this solvent, a quantity of ferrocene was injected into the cell, sufficient to bring its concentration up to ca. 10^{-3} M, and the cyclic voltammogram for its oxidation recorded using a separate Pt working electrode.[15a–c] Salts used as supporting electrolytes were obtained in the highest possible purity from Fluka or Aldrich and used without further purification.

Spectroelectrochemical studies were carried out with the cell mounted in the sample compartment of an HP8452A diode array spectrometer with the light beam fully blocked by the active electrode area (ITO and Pt electrodes). Spectra were recorded at periodic intervals during slow cyclic voltammetric (CV) sweeps, or absorbance/time data acquired during CV experiments, or after application of potential steps. Absorptivities and dichroism of the neutral and oxidized PcPS films (ITO and quartz substrates) were obtained in a Perkin-Elmer Lambda 9 spectrophotometer, outfitted with polarizing optics. The quartz or ITO substrate samples, overcoated with 40–80 layers of PcPS, were characterized in this system before and after chemical or electrochemical oxidation of the PcPS films.

XPS experiments were conducted using a Vacuum Generators MKII ESCALAB, AlKα source operated at 300 W. The PcPS samples studied were each 22 ML on ITO. Samples were immersed in aqueous 0.1 M $LiClO_4$. The electrochemically oxidized films were then potentiostated at the voltages discussed in the text, while the control film was immersed in the same solution without connection to the potentiostat for the same time as used for the oxidation experiments. Upon attainment of steady-state conditions in the potentiostated film, which corresponded to the lack of any additional change in faradaic current, the samples were emmersed under potential control, dipped once in ultra pure H_2O for ca. 10 s, and then immediately mounted

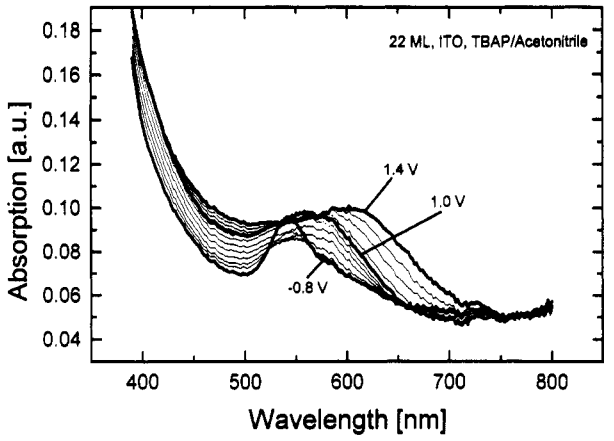

Figure 2. Absorbance spectra for a 22 ML PcPS/ITO electrode poised at potentials of −0.8 V, +1.0 V, and +1.4 V (dark lines). Faint lines are used to show spectra recorded at intermediate potentials. Identical absorbance spectra were recorded during the return of the PcPS film to the neutral form.

on the appropriate sample holder and moved into the vacuum system. The control PcPS/ITO electrode was subjected to the same rinsing step prior to insertion into the vacuum. Samples were examined at the normal takeoff angle for the analyzer/lens (ca. 0 °C to the sample normal) and at takeoff angles which maximized surface sensitivity of the XPS data obtained (ca. angles as high as 75° were used). All data were background corrected according to established procedures[16] and the intensity ratios reported corrected for differences in ionization cross section, escape depth, and analyzer transmission function.

ESR experiments were performed with a continuous-wave x-band spectrometer ESP 300 and an electrochemical cell made of Quartz type WG-810-A-Q, both made by Bruker.[17] The cell was configured with a Pt wire as counter electrode, a Ag/AgCl (AgCl coated silver wire) as reference electrode, and a Pt wire dip coated with multiple layers of PcPS as working electrode. The electrolyte for these ESR experiments was a 0.1 molar solution of tetrabutylammonium perchlorate in acetonitrile. To cover the working electrode wire with a PcPS thin film, a dilute solution of PcPS (2 mg PcPS in 10 mL of chloroform) was dropped on the wire and the solvent evaporated. The working electrode was then inserted in the cell filled with electrolyte while dry nitrogen was bubbling continuously through the solution. The cell was built into the spectrometer in such a way that the flat part of it was situated in an "electromagnetic knot" of the cavity. The cell potential was stepped to distinct values, and ESR spectra were recorded when steady-state currents had been reached at each potential. Following these experiments the electrochemical cell was removed from the spectrometer cavity and the spectrometer was calibrated (both for g value and spin density) by characterizing a known amount of a calibration standard (4-oxo-2,2,6,6-tetramethylpiperidin-1-oxyl).

Results and Discussion

PcPs Oxidation in CH_3CN Spectroelectrochemical Characterization. Figures 2 and 3 show the voltammetry and spectroelectrochemistry of a 22 ML PcPS/ITO film in CH_3CN, 0.1 M TBAP. The voltammetric data (Figure 3a) show two broad oxidation waves at potentials positive of 0.0 and 0.4 V, respectively (the first wave can be ±50% of the intensity shown in Figure 3a, for various PcPS films), a decline in current positive of 0.65 V, and then the resumption of current flow positive of 0.8 V, until the most positive potential obtainable for these films in this solvent was reached at ca. 1.4 V. The oxidation waves seen in the region between 0.0 and 1.0 V were accompanied by symmetric reduction waves on the return sweeps, provided low voltammetric sweep rates were used (≤5 mV/s). Systematic changes were seen for the absorbance spectrum of PcPS during these oxidation processes (Figure 2) which, along with coulometric analysis (see below), suggest that the first two oxidation waves (up to +1.0 V)

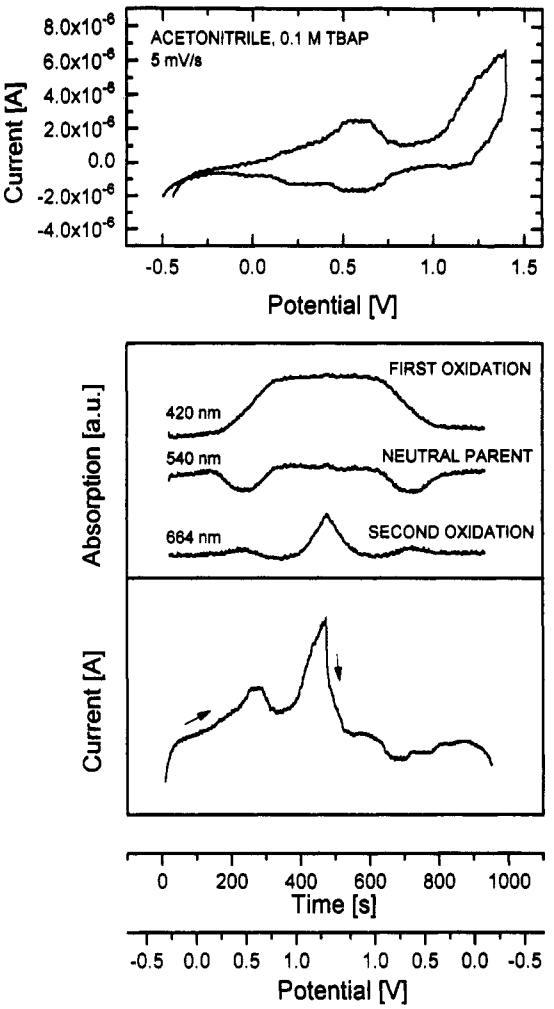

Figure 3. (Top) voltammogram for a 22 ML PcPS/ITO thin film in CH_3CN, 0.1 M TBAP; (middle) absorbance changes versus potential (and time) data obtained at 420, 540, and 664 nm during the oxidation and reduction cycles of the voltammogram shown in the upper panel; (bottom) the voltammogram in the upper panel redisplayed as current versus time to align with the spectroelectrochemical data of the middle panel. Derivatives of absorbance change versus change in potential ($\Delta A/\Delta E$), computed from the data of the middle panel, were comparable in form to the current versus time data of the lower panel (see text).

result from the same oxidation chemistry and, at a potential of ca. 1.0 V, reflect the oxidation of nearly each Pc ring in the polymer thin film. The oxidation process positive of 1.0 V appears to reflect the onset of a second, distinct process and appears to correspond to the removal of a second electron from at least a portion of the already oxidized Pc rings. Attempts to reduce these films in CH_3CN were not successful—scanning the electrode potential to ca. −2.0 V did not produce distinguishable voltammetric waves, as would be expected from previous voltammetric studies of SiPc digomers,[15] and did not produce changes in absorbance spectra. Degradation of the PcPS film was noted after prolonged exposure to such negative potentials.

The absorbance spectrum of the neutral form (−0.8 V) of the PcPS 22 ML/ITO film (Figure 2a) is identical in shape to spectra seen for thicker PcPS films on quartz substrates (see below). The Q-band spectrum for the phthalocyanine chromophore is blue shifted to ca. 540 nm versus the solution monomer absorption maximum at ca. 690 nm. Such shifts have been discussed before for crystalline SiPc polymers, the PcPS system, 2–4 unit oligomeric forms of polymerized SiPc, and related crystalline, linear cofacial stacks of AlPc-F and AlPc-Cl.[6,11c–e,15b,c,18,19] The linear cofacial arrangement of the

Table 1. Coulometric and Spectroscopic Analysis of Typical PcPS Thin Film Oxidations

sample	Q_T (μC/cm^2)	Q_f (μC/cm^2)	Q_f/Q_{th}[a]	$\Delta A_{420,440nm}$	$(\Delta A_{obs}/\Delta A_{th})$[b]
22 ML/ITO[c]					
0.3 V	141	100	0.24	0.008_3	$0.2_4 \rightarrow 0.3_8$
0.8 V	457	326	0.79	0.022_0	$0.6_7 \rightarrow 1.0$
1.0 V				0.024_2	$0.7_4 \rightarrow 1.1$
22 ML/ITO[d]					
0.8 V	415	340	0.82	0.022_0	$0.7_6 \rightarrow 1.1$
1.0 V	371	229	0.55	0.025_0	$0.6_7 \rightarrow 1.0$
22 ML/ITO[e]					
0.8 V	453	256	0.61	0.017_3	$0.5_2 \rightarrow 0.7_9$
5 ML/Au-MPOTE/	86	55	0.59		
11 ML/Au-MPOTE/	211	158	0.76		
21 ML/Au-MPOTE/	321	243	0.61		

[a] Q_{th} assumes a faradaic charge of 18.8 μC/cm^2 per monolayer of PcPS for the one-electron oxidation of each Pc unit in the film. [b] Assumes an absorptivity at the indicated wavelengths, for the first oxidation product of PcPS, of $0.001_0 \geq \beta_{420,440nm} \geq 0.001_5$ ML^{-1}. [c] HMW (HMW = high molecular weight version of PcPS), not annealed before characterization, 0.15 M TBAP/CH_3CN, scan rate 5 mV/s. [d] HMW, annealed at 150 °C for 8 h before characterization; all other characterization parameters as for *a*. [e] HMW, not annealed, 0.1 M $LiClO_4$/pH = 6.5, H_2O; all other characterization parameters as for *a* and *b*. [f] HMW, not annealed, 0.1 M $LiClO_4$/pH = 6.5, H_2O, coulometric analysis includes polarization out to 0.8 V.

Pc rings, with a ring-to-ring separation of ca. 3.3 Å, forces the transition dipoles to couple in a parallel configuration, causing significant exciton splitting in the Q-band and making the higher energy optical transition allowed.[6a,20] The tail seen on the low-energy side of this Q-band spectrum arises in part from (a) other allowed optical transitions, arising from orientational disorder among the rings stacked along the polymer chain and (b) from small percentages of lower molecular weight oligomeric forms of PcPS, known to be present in these assemblies (see below) after completion of the polymerization steps. These oligomeric forms are variable in their concentration, depending upon the reaction conditions used to form the PcPS polymer, but generally comprise less than ca. 5% of the electrochemically active Pc in the thin film.

Spectra of the PcPS/ITO, Au, Pt thin films were recorded throughout the oxidation and reduction sweeps, but only those at selected potentials are shown for clarity in Figure 2. The spectrum for the electrode poised at 0.8 V is similar in shape to those seen at less positive potentials and represents the full development of a new spectral peak centered at ca. 580 nm and the loss of the original Q-band peak. The spectrum is close in appearance to Nujol-mull powder spectra reported for I_2-oxidized versions of crystalline SiPc polymers.[11c-e] Reduction of the PcPS film after polarization to 1.0 V restored 100% of the original reduced PcPS film spectrum. If the potential was next scanned to ca. 1.4–1.5 V, another new broad spectrum appeared, with a peak centered at ca. 615 nm.

Despite the width of these absorbance bands, there are distinct regions where all of the redox species can be resolved. From 420 to 470 nm on all of the electrode materials there is little or no optical density from neutral PcPS, this is a region where the first oxidation product absorbs uniquely. Likewise, the region near 648 nm is free from absorption of both the neutral and first oxidation product of PcPS and from optical aberrations which accompanied potential changes at the ITO and Au electrodes. Decreases in the 540-nm band intensity can be used to indicate the onset for loss of parent neutral PcPS; however, overlap with the product peak(s) brings its intensity back up later in the voltammogram. The absorbance versus potential in these three wavelength regions, along with the absorbance change at 540 nm, are shown accompanying the CV curve in Figure 3.

At the onset for oxidative current the initial loss of neutral PcPS is shown clearly by the attenuation of the 540-nm band and the immediate onset for absorbance at 420–470 nm. At the plateau of current in the first oxidation process (0.3 V), and the onset of the second wave (0.4 V), there is virtually no difference in the rate of change of $A_{420-470nm}$. No new spectral band is seen at this potential, and the constant rate of change of $A_{420-470nm}$ up to 0.6 V suggests that the product of the oxidation process at 0.6 V is the same as at lower potentials. As the current decays positive of 0.6 V, the rate of change of $A_{420-470}$ diminishes, consistent with diffusion/migration control of the oxidation process, as suggested by the CV curve. The additional increase seen in $A_{420-470nm}$ positive of 0.8 V is due to overlap with the spectrum of the next oxidation product, and this overlap was minimized by observing absorbed changes only at 420 nm. Positive of 0.9 V the absorbance at 648 nm rises sharply along with the oxidation current. The absorbance changes observed on the oxidative sweep (out to ca. 1.4 V) are reversed by immediately scanning the potential negatively, suggesting conservation of the PcPS chromophore. *Prolonged* exposure of the film to potentials positive of 1.0 V did cause the loss of a few percent of the chromophore.

Table 1 shows the results of combined optical and electrochemical analysis of the oxidation of typical PcPS films on ITO. Comparable coulometric results were obtained for PcPS films on Au and Pt, and comparable spectroelectrochemical data were obtained for the oxidation of PcPS films on Pt. The absorbance/voltage data and the CV curves had to be used in combination to give reasonable estimates of the extent of oxidation of the Pc units within the PcPS thin film. The faradaic currents in voltammograms like that in Figure 3 were approximately resolved from the capacitive current contribution by assuming that the current flowing at 0.8 V was entirely capacitive (i_{cap}) and that the capacitive current in the region between 0.0 and 0.8 V was proportional to the total current, yielding a sigmoidal i_{cap} versus voltage function, like that observed for conductive polymer films in refs 20 and 21. It is recognized, however, that currents in the oxidation of polymer thin films are limited by rates of electron transport, counterion transport, solvent permeation, etc., and are rarely so well behaved as to permit unambiguous differentiation from the capacitive current using the cyclic voltammogram alone.[21-23] The spectral data like that shown in Figure 3 were used to help indicate when faradaic current flow in PcPS film oxidation had ceased or had reached diffusion control. $\Delta A/\Delta E$ derivatives of the absorbance versus potential data were consistently analyzed, and since these derivative functions parallel *only* the flow of faradaic current, they were used to find the points where apparent diffusion control began or where

capacitive current flow dominated the electrochemical process and could be removed to improve the estimate of faradaic charge, Q_f.

The value of Q_{th} used in computing Q_f/Q_{th} is the charge assumed for complete oxidation of each Pc unit by one electron—18.8 $\mu C/cm^2$ per monolayer, based upon the projected area per molecule of 85 $Å^2$ and the assumption of a constant density per monolayer.[6] For the coverages of PcPS used to compute these charge ratios it is known from X-ray characterization of comparable annealed PcPS films that these rodlike polymers are arranged in hexagonal closest packed configurations on the substrate surface, with the rod axis parallel to the substrates. It is the spacing between polymer rods, obtained from this same X-ray data, which was used to confirm the projected area per molecule. This area is also consistent with areas computed from the LB pressure–area isotherms and confirms that the Pc rings are stacked perpendicular to the plane of the substrate.[6]

The absolute absorbance changes during these voltammograms, or absorbance changes induced by potential step experiments, also gave some idea of the extent of PcPS oxidation versus potential. In the absence of absorptivity data for the thin film oxidation product of PcPS we assume that the probability for the Q-band $\pi \rightarrow \pi^*$ transitions for both the neutral PcPS and the oxidized product, are equal. The absorbance spectra of the PcPS films in CH_3CN/0.1 M TBAP, at –0.5 and 1.0 V, and from comparable spectra were taken for neutral PcPS, and the oxidized form was created from treatment of these same films in aqueous BrO_3^- (see below) and corrected for background absorbances. We were able to estimate an absorptivity per equivalent monolayer of oxidized PcPS, at 420–470 nm (for 40–80 ML films) of between 0.001_0 and 0.001_5 ML^{-1}. ML^{-1} is an equivalent monolayer absorptivity and assumes constant density of the LB–PcPS monolayers, regardless of total film thickness. Using these assumptions the number of equivalent monolayers of PcPS experiencing oxidation was computed, and typical values are listed in Table 1. The observed absorbance changes versus those expected for complete oxidation of the PcPS film by one electron ($\Delta A/\Delta A_{th}$) were also computed, which proved to be quite comparable to the Q_f/Q_{th} values. From Table 1 it can be seen that the first plateau in the voltammetric oxidation of these PcPS films occurs when the PcPS film has reached 20–30% of the total charge expected for full oxidation of each Pc ring, i.e., the stoichiometry of the film is describable as $Pc^{+x}(ClO_4^-)_{x=0.2\rightarrow0.3}$. Upon reaching 0.8 V the extent of oxidation appears to have increased to $x \geq 0.6$, with a realistic range being $0.6 \leq x \leq 0.8$.

As previously demonstrated for other electrochemically active polymer thin films, potential step experiments were used in conjunction with absorbance changes to estimate the effective diffusion rate of charge.[1-4,21] The faradaic current flow (i), in response to a potential step, can be written in terms of the thickness of the PcPS thin films (x), the maximum concentration of electroactive sites (C_s), the apparent diffusion coefficient, D_{app}, which is known to be a combined constant reflecting both electron self-exchange and ion migration rates, the time after application of the potential step (t), and other usual electrochemical parameters:

$$i = nFAD^{1/2}\pi^{-1/2}C_s t^{-1/2}[1 + 2\sum_{k=1}^{\infty}(-1)^k \exp(-k^2L^2/Dt)] \quad (1)$$

The integral form of this relationship, which reflects the absorbance/time relationship, written in an adimensional

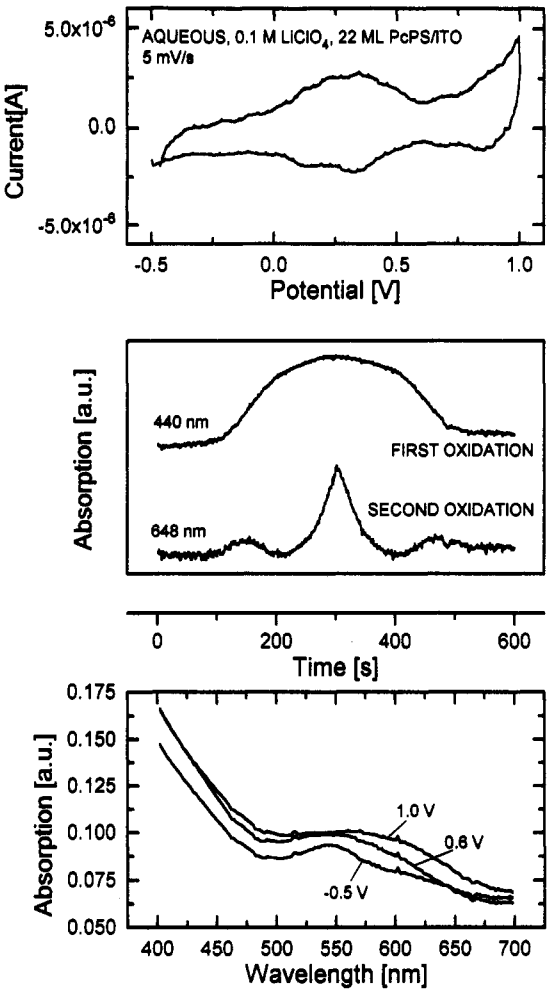

Figure 4. (Top) voltammogram for a 22 ML PcPS/ITO thin film in contact with H_2O, 0.1 M $LiClO_4$; (middle) absorbance changes versus potential (time) during the oxidation and reduction cycles of that film; (bottom) absorbance spectra captured at potentials of –0.5 V, +0.6 V, and +1.0 V.

form, allows for the estimation of D_{app} from the time ($t_{3/4}$) necessary to reach 3/4 of the steady-state absorbance after the potential step, the film thickness, x, and the parameter $T_{3/4} = 0.51$, obtained from a generalized working curve describing this type of electrochemical process:

$$D_{app,(cm^2/s)} = T_{3/4}\frac{x^2}{t_{3/4}} \quad (2)$$

For the 22ML films described above, in CH_3CN, potential steps to between 0.5 and 0.8 V were characterized, with the finding that the D_{app} values were (1–2) × 10^{-11} cm^2/s for the oxidation of the PcPS films and (6–7) × 10^{-11} cm^2/s determined from the optical changes noted during reduction of the oxidized films. These values of D_{app} are at the low end of the scale seen for ion/electron migration rates in conductive or ion-exchange-like polymeric media[1-5] and reflect the difficulty of ion migration in these highly densified PcPS thin films.

Oxidation of PcPS Thin Films in Aqueous Media. Figure 4 shows the voltammetry of a 22 ML PcPS/ITO film in contact with aqueous 0.1 M $LiClO_4$, the absorbance spectra at selected potentials, and the absorbance versus potential data for selected wavelengths. Near pH = 7 the voltammetric oxidation of the PsPS film in aqueous media is similar to that behavior seen in CH_3CN, both with regard to the shape of the voltammograms and the absorbance spectra of the products. Starting at ca. 0.0 V the onset of

oxidative current is paralleled by a drop in the absorbance at 540 nm and the growth of a new band, centered at ca. 580 nm, with the corresponding increases in spectral intensity at 420–470-nm versus potential, as were seen in CH_3CN discussed above. Between 0.0 and 0.8 V the change in absorbance at those wavelengths leads to a predicted conversion of ca. 50–80% of PcPS to the oxidized product, or $\Delta A_{obs}/\Delta A_{th} = 0.5 \rightarrow 0.8$ (Table 1). The shape of the CV curves suggests that this oxidation process is compressed into a window ca. 600 mV wide, as opposed to the 800 mV span seen in CH_3CN. If the direction of potential scan was reversed at this point, both the coulometric and spectroelectrochemical data suggest complete conservation of PcPs, over multiple cycles (see below).

At ca. 1.0 V the process leading to the first oxidation product ceases, and there is a clear onset for a new spectral feature absorbing at longer wavelengths than 580 nm and shown by the increase in absorbance at 648 nm in Figure 4. We were unable, however, to hold the potential positive enough in H_2O to capture spectra for the PcPs dication form of the quality of those shown in Figure 2, without loss of the PcPS film. Despite the lower stability of the second oxidation product of PcPS the rate of change of these spectral features versus potential confirms a commonality of the two PcPS oxidation processes with those seen in the nonaqueous oxidation. Coulometric data in Table 1 show that the extent of oxidation at 0.8 V in H_2O is only slightly less than that achievable in CH_3CN. Potential step experiments were also conducted in these aqueous studies, as discussed above, for the estimation of D_{app}. Using ClO_4^- as the supporting electrolyte, values of D_{app} for 22 ML PcPS films were found to be in the range of $(0.5–1.0) \times 10^{-11}$ cm^2/s for both oxidation and reduction processes, somewhat smaller than seen for the same processes in acetonitrile.

In preparation for the XPS experiments described below the open circuit potentials of 22 ML PcPS/ITO films were monitored as a function of time in the 0.1 M $LiClO_4/H_2O$ solutions, after potential steps to specified voltages. At each potential, the system was allowed to oxidize and stabilize for several minutes, and the cell moved to open circuit, leaving the electrode free to achieve a rest potential versus the Ag/AgCl reference electrode. When the electrode was allowed to achieve equilibrium under potential control over ca. 5 min at 0.1 V, the decay in the subsequent open circuit potential was less than 1% (to lower potentials) in 5 min. At 0.3 V the decay in 5 min was ca. 7%, at 0.4 V it was ca. 8%, and for an electrode equilibrated at 0.8 V and then disconnected, the potential had decayed by ca. 30%, 5 min following open circuit. There was a striking increase in the rate of this open circuit potential decay when the electrode was polarized positive of 0.5 V, which is near the point on the voltammograms where the faradaic current is subsiding, before the onset of the second oxidation process. The decay of this open circuit potential is consistent with partial reduction of the oxidized PcPS film, accompanied by loss of counterion. This loss is confirmed below.

Oxidation of the PcPS film could also be achieved with water-soluble solution oxidants such as BrO_3^-, IO_3^-, etc. PcPS films on quartz (Γ_{PcPS} = 80 ML) were oxidized by immersion in aqueous BrO_3^- (0.1 M, pH = 2) for periods up to 36 h. The extent of oxidation after a 36-h exposure to the BrO_3^- solution appeared to be the same as for electrodes polarized to ca. 0.8 V in both H_2O and CH_3CN. Solution oxidation of these thicker PcPS films on quartz substrates allowed the measurement of the absorbance spectrum of the neutral and oxidized forms for both parallel and perpendicular polarization of light. For both the reduced and oxidized forms of the PcPS thin film, provided that annealing of the film had been carried out after LB-deposition (see below), $A_\perp/A_\parallel$ = 3.05. This ratio is consistent with those determined in previous studies of PcPS thin films[6a,i] and yields an order parameter S = ca. 0.51 for both the oxidized and reduced forms of PcPS. This result suggests that, while there must be clear incorporation of high local concentrations of counterion during oxidation, there is little change in the ordering of these films during oxidation, assuming that the $\pi \rightarrow \pi^*$ optical transition of the oxidized Pc still lies mainly in the plane of the Pc ring.[6i]

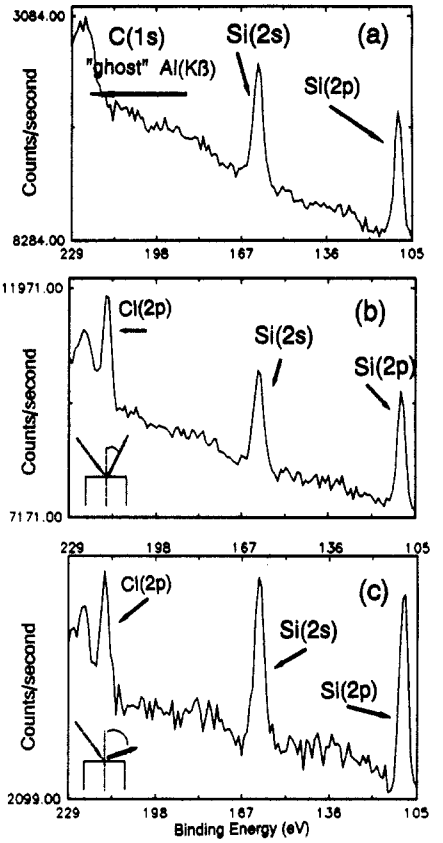

Figure 5. X-ray photoelectron spectra of PcPS/ITO thin films; (a) PcPS thin film in the neutral state, after immersion and emmersion in the $H_2O/LiClO_4$ electrolyte, but without polarization; (b) a similar electrode after polarization at +0.5 V, XPS data taken at near normal sample/analyzer takeoff angles to maximize subsurface information; (c) the same electrode as in b where the XPS spectrum was recorded with a high sample/analyzer takeoff angle to maximize surface sensitivity (note the lower apparent Cl content of the near surface region in this spectrum).

XPS Analysis of the Aqueous Oxidation of PcPS Thin Films. Figure 5 shows three XPS spectra for (a) a control 22 ML PcPS/ITO thin film and (b and c) a 22 ML PcPS/ITO film which had been polarized to 0.5 V, allowed to equilibrate for ca. 5 min, removed from solution under potential control, dipped in pure water for ca. 30 s, and then immediately inserted into the UHV surface analysis system. The low- and high-resolution spectra of the control showed the lack of any elemental components other than those expected for PcPS (C, N, Si, and O), with barely detectable levels of Cl which may have been incorporated from the SiPc monomer. The C/N and N/Si ratios were within a few percent of those expected for PcPS. Following oxidation at potentials positive of 0.5 V, both the N(1s) and C(1s) spectra were broadened to the high-binding energy side, consistent with the formation of oxidized Pc rings, and removal of electrons from the HOMO regions

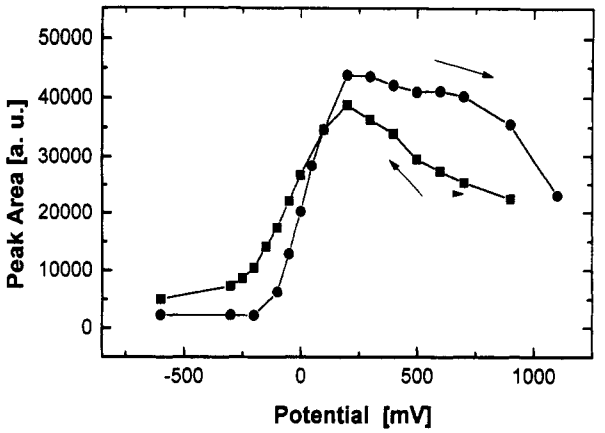

Figure 6. Electron spin resonance signal intensity versus potential for a PcPS thin film coated over a Pt wire, inserted into an electrochemical cell in the ESR cavity. Arrows indicate direction of potential scan. The apparent loss ESR signal (assumed to be due to loss of PcPS) during the reduction cycle could be avoided by polarizing to ca. 0.8 V instead of +1.0 V.

of those molecules.[16b,24] Because of the high concentration of hydrocarbon side chains, the N(1s) spectra, representing the Pc ring only, were more significantly affected by this oxidation process.

Figure 5a shows the Cl(2p), Si(2s), and Si(2p) spectral regions for the control PcPS film, which saw electrolyte and H_2O rinse, but was not polarized. An additional peak is seen due to a C(1s) transition, which appears as a result of Mg(Lβ) satellite radiation from the nonmonochromatized X-ray source. Following oxidation of a PcPS/ITO film at 0.5 V, and at an analyzer/lens takeoff angle for the photoemitted electrons of 0°, versus sample normal, the spectrum in Figure 5b results. From the background corrected version of this spectrum the Cl(2p)/Si(2s) and Cl(2p)/Si(2p) relative atomic ratios were computed, following correction for differences in ionization probability for these transitions, escape depth of the photoelectrons, and analyzer/lens transmission functions.[16a] For this takeoff angle the Cl/Si ratios varied from 0.32 to 0.35. Figure 5c shows the same sample at a much higher takeoff angle (75°), which improves the surface sensitivity of this technique.[16b] At this takeoff angle the Cl/Si ratios were both ca. 0.22. The lower ratio at this higher takeoff angle is anticipated, since it reflects the unavoidable loss of perchlorate in the near-surface region after emersion and rinsing of the film. Assuming that the diffusion rate of ClO_4^- from deep in the PcPS film was slow, that the ClO_4^- was distributed uniformly throughout the film immediately following oxidation, and that the angular-dependent XPS data reflect a lower limit to the perchlorate content, we estimate that the Cl/Si ratio (perchlorate stoichiometry) of the PcPS film oxidized at 0.5 V is ca. 0.5; i.e., the PcPS composition is $(PcPS)^{+0.5}(ClO_4^-)_{0.5}$. This stoichiometry at 0.5 V is consistent with both the analysis of faradaic currents and absorbance changes given in Table 1.

ESR Experiments. Oxidation of the dip-coated PcPS films on Pt in CH_3CN showed an ESR signal (g = 2.003 ± 0.002, FWHM = 9 MHz) which increased in magnitude at potentials consistent with the spectroelectrochemical oxidation of the LB films discussed above (Figure 6). As expected, if the product of the initial oxidation process is the Pc cation radical, the integrated ESR peak area, plotted versus the applied potential, increases most rapidly during the initial oxidation of the PcPS film and reaches a plateau near 0.5 V. At more positive potentials there is a loss of ESR signal. Provided that the potential of this electrode was kept below 0.8 V, it was possible to cycle the potential back and forth through this oxidation region without significant loss of ESR signal. Potential excursions positive of 0.8 V did result in some loss of ESR signal during the subsequent reduction cycle (Figure 6). Since it is a reversible process, we believe the loss of ESR signal positive of 0.5 V to signal the onset of a diamagnetic species such as dications of SiPc, for which there should not be an ESR response.[11,17] Although these experiments were not conducted on the highly ordered LB films of the other experiments, there appears to be a clear indication of the formation of $Pc^{\bullet+}$ cation radical species in these films during the initial oxidation process, precisely that expected from previous studies of the crystalline forms of SiPc polymers.[11]

Oxidation Processes for Low Molecular Weight Oligomeric Thin Films of PcPS. It was also possible to carry out aqueous oxidation and spectroelectrochemistry of PcPS–LB thin films created from low molecular weight oligomeric forms of PcPS (mainly dimers of SiPc, see above). In aqueous ClO_4^- the onset for the first oxidation process for the oligomer films occurred at ca. 0.2–0.3 V, which is more positive of the onset for oxidation of the polymer by at least 0.2 V. This shift in the first oxidation potential is consistent with the differences in first oxidation potential seen previously for cofacially stacked SiPc oligomers and SiNPc oligomers which have been explored in solution soluble forms.[6a,15] The interaction between closely spaced Pc rings is known to shift the first oxidation potential of these molecules by up to 0.6 V, as one proceeds from the simple monomer to the dimer and trimer in this series. These shifts correlate with the shifts in both gas-phase and solid-state first ionization potentials[25,26] and with the shifts in the Q-band spectra, as discussed below. From this voltammetric data we were able to determine the potential window in which to expect oxidation currents for oligomeric impurities in the normal PcPS films. From the voltammetric properties of the high molecular weight PcPS films explored here, and the spectroscopic characterization of these films, we judge the amount of dimeric or trimeric forms of the SiPc polymer in these PcPS films to be less than a few percent and likely not significant in the electrochemical processes discussed above.

The oligomeric PcPS thin films showed an absorbance band of the neutral form maximized at ca. 640 nm. The oxidized form of the oligomeric PcPS thin film showed a broad band, maximized near ca. 580 nm, quite close to the band seen for the first oxidized form of the high molecular weight PcPS thin films (Figure 2). There was also a striking attenuation of the absorbance seen for the neutral oligomer PcPS film in the region between 650 and 800 nm, where monomeric forms of closely packed PcPS are expected to be detected. The attenuation of absorbance in this spectral region, and the similarity of the spectrum of the oxidized oligomeric mixture and that of the PcPS high molecular weight polymer, suggest that the optical transition for the cation PcPS arises from a strongly localized chromophore, whose interactions with neighboring Pc units is much weaker than in the case of the neutral molecule; i.e., there is little exciton splitting in the cation form of the Pc versus the neutral form.

Electrochemical Stability and Dependencies of Electrochemical Reactivities on Coverage, Sweep Rate, and Post Deposition Annealing and Tests for Film Porosity/Redox Mediation. Figure 7 (lower panels) shows the cyclic voltammetric behavior of a 1 ML PcPS film on the Au-MPOTE, at the end of the first cycle, 1000 cycles, and 15 000 cycles. There is some enhancement of the oxidative and reductive peaks after the first few

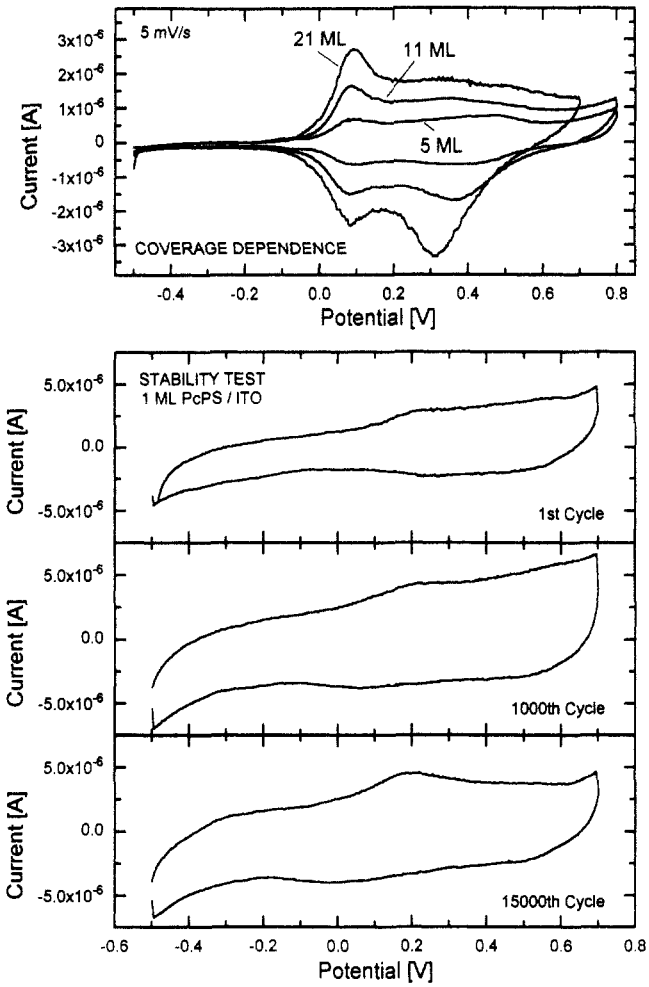

Figure 7. (Top) cyclic voltammograms (sweep rate of 5 mV per s) of PcPS/Au thin films in H_2O at coverages of 5, 11, and 21 ML; (bottom) cyclic voltammograms of 1 ML PcPS/ITO thin films after 1, 1000, and 15 000 full cycles between −0.5 and +0.7 V.

cycles and then essentially constant electrochemical behavior following that. This stability is reflected in the films of higher coverage, on all substrates, and in all nonaqueous and aqueous electrolytes that we have explored.

The voltammograms in Figure 7 (upper panel), from typical PcPS films at 5, 11, and 21 ML coverages, show the manner in which the oxidative currents scale with coverage (see also Table 1). The initial oxidation peak is enhanced in these lower pH electrolytes, as is discussed further below. There is some difficulty, as noted above, in resolving the true faradaic charge, Q_f, from the capacitive charge, Q_c, in these voltammograms and in the voltammograms for the 1 ML films. Plots were made of reasonable estimates of Q_f versus Γ_{PcPS} for films above 3 ML in coverage and $Q_T = Q_f + Q_c$ versus Γ_{PcPS} for all films, including the 1 ML coverages. In both cases linear relationships were observed, and for the Q_T versus Γ_{PcPS} plots, zero intercepts observed.

Figure 8a–d shows the effect of sweep rate on the shape of the voltammograms for an 11 ML/Au PcPS film in aqueous 0.1 M $LiClO_4$, and is typical of the behavior seen for all PcPS films examined in most aqueous solvents. At sweep rates less than 5 mV/s the onset for oxidation occurs with a clearly distinguished peak, followed by the poorly resolved additional oxidation process discussed above. The spectroscopic experiments described above show that these multiple oxidation waves, out to potentials of ca. 0.8 V, represent the same basic $Pc \rightarrow Pc^{\bullet+} + e^-$ oxidation chemistry. Upon sweep reversal the reduction of the $PcPS_{ox}$ film is carried out in two clearly resolved steps. The position of the most positive reduction peak is strongly dependent upon sweep rate (Figure 8) and shifts negatively by over 200 mV when the sweep rate is increased from 1 to 100 mV per second. This reduction peak also shifts negatively for experiments where the sweep rates are held constant and where the PcPS coverage is systematically increased (e.g., Figure 7b, top panel).

The most negative reduction peak (at ca. 0.1 V) is not significantly influenced by sweep rate or PcPS coverage. The resolution of the oxidation/reduction behavior of these PcPS films into kinetically facile and kinetically limited processes, associated with the same basic redox chemistry, is consistent with the presence of two or more different electrochemical domains in these PcPS films. Behavior similar to this has been seen previously for much thicker electrodeposited polymer films which are oxidatively doped and is expected for films with domains which cannot achieve electrochemical equilibrium with the substrate electrode during the time course of the experiment.[1a,b,2-4]

We hypothesize that the first domain exhibits oxidation and reduction of the film with facile electron and ion transport—the second domain exhibits a broad range of oxidation and reduction potentials due to a combination of restricted ion and electron diffusion. Upon oxidation there appears to be a redistribution of charge in the second domain. Reduction of PcPS within that domain is strongly influenced by anion expulsion rates (which are presumed to be slow), the thickness of the PcPS film, and the time domain of the voltammetric experiment. It has also been recently shown that the reduction of oxidatively doped polymer films is likely accompanied first by cation incorporation to achieve electroneutrality and the subsequent diffusion of both cations and anions out of the neutral film (see below).[1-4,22] Solvent permeation and efflux can also be an important factor determining rates of oxidation and reduction.[4]

This hypothesis of domain formation gains support in Figure 8e,f where the electrochemical behavior of 11 ML PcPS/Au films in 0.1 M $LiClO_4$ is compared. Figure 8e shows the voltammetry of a film examined immediately after LB deposition, while Figure 8f shows the effect of annealing the same type of film at ca. 120 °C for 8 h following the LB deposition. The most notable effect of annealing these films is in the attenuation of oxidation and reduction currents in the region near 0.1 V, suggesting alteration of the domain for which redox activity was most facile in the unannealed (least ordered) film. The sweep rate dependence of peak position for the most positive reduction peak persists after annealing, suggesting that the electrochemical activity in this potential region corresponds to PcPS that was well ordered at deposition and not subject to further changes upon annealing. Annealing of the PcPS films has been shown previously to significantly enhance the ordering of these films, where $A_\perp/A_\parallel$ for the absorbance peak at 540 nm was increased from ca. 2.3 to 6.0 by such prolonged heating. This change in polarization ratio corresponds to an increase in the ordering parameter of these films from 0.39 to 0.71.[6a,i] We have seen similar changes in these studies for the films made on quartz (see above). We now believe that the most negative oxidation/reduction peaks for freshly deposited LB PcPS layers correspond to electron transfer in the PcPS environments which are less ordered and more easily equilibrated with the electrode potential.[1] It is interesting that the magnitude of current flowing in the potential region near 0.1 V, for the unannealed films, scales with Γ_{PcPS}, which suggest that this process cannot be only

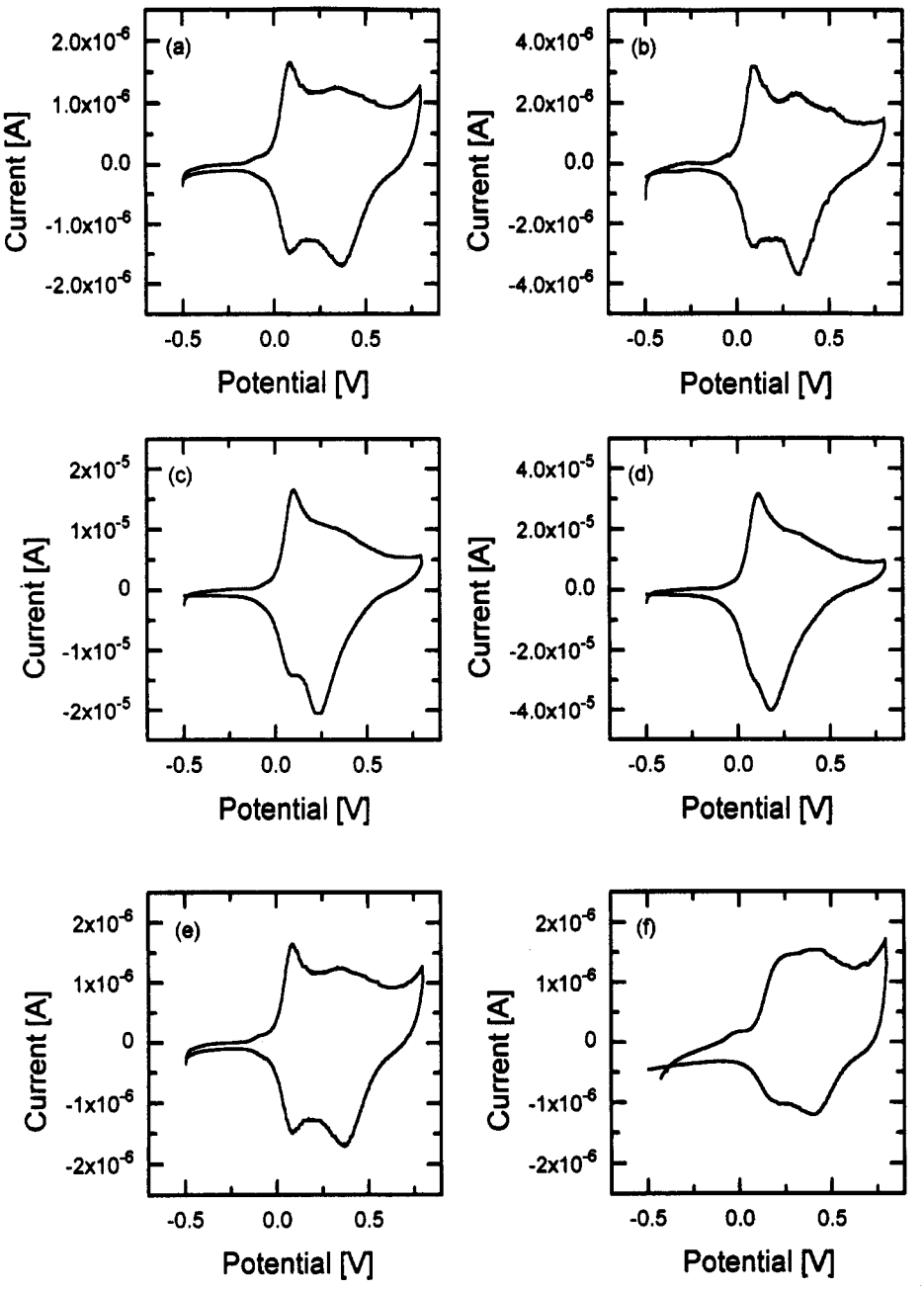

Figure 8. (a–d) Cyclic voltammograms of a 22 ML PcPS/Au thin film in contact with H_2O at sweep rates of 5, 10, 50, and 100 mV/per s, respectively; (e and f) similar voltammograms at 5 mV/s for films freshly prepared and annealed for 8 h at 150 °C, respectively.

associated with loosely bound PcPS near the electrode or electrolyte interface.

Figure 9 shows the voltammetric responses for 3 ML PcPS/Au films in normal aqueous electrolytes and in aqueous electrolytes with millimolar concentrations of either ferrocene or ferrocyanide. Down to a PcPS coverage of 3 ML the PcPS films proved to be quite densely packed and impenetrable to solution species such as hydroquinone, ferrocyanide, and ferrocene. The normally facile oxidation of Fc to Fc^+ (near 0.0 V) at bare gold electrodes, in water (ca. 10% $MeOH/H_2O$, 0.1 M HNO_3) (Figure 9c), is impeded at its $E^{\circ\prime}$ by the PcPs layers ($\Gamma_{PcPS} \geq 3$ ML), as is the oxidation of the added MeOH (near +0.5 V) (Figure 9d). The peak current for the initial oxidation of the PcPS film was enhanced over that seen in solutions missing the ferrocene (Figure 9b), presumably due to the electrocatalytic regeneration of neutral PcPS. The oxidation peak due to $Fc \rightarrow Fc^+ + e^-$ on the PcPS-modified Au surface proceeded only at potentials positive of the initial oxidation of PcPS, where the PcPS film was presumably made conductive (Figure 9d). Upon sweep reversal, the reduction of the Fc^+ formed on the oxidative sweep (which would normally occur near 0.0 V) was blocked by the reduction of the $PcPS_{ox}$ film back to the neutral form of PcPS (near +0.2 V), rendering the film incapable of supporting the charge transport necessary to carry out that reduction. Similar rectification of electrochemical oxidation/reductions were obtained for 1–100 mM concentrations of hydroquinone and ferrocyanide. Where the formal potential for the solution soluble species is positive of 0.4 V (e.g., iron o-phenanthroline), both the oxidation and reduction occurred on the PcPS films ($\Gamma_{PcPS} \geq 3$ ML) with rates at or exceeding those seen on bare Au.

Conclusions

The electrochemical oxidation of PcPS thin films occurs over potential ranges which are consistent with those expected from previous studies of monomer and oligomer silicon phthalocyanine polymers which had been solubilized by alkyl end groups[15] but show some differences with previous studies of the crystalline SiPc polymer and the tera-*tert*-butyl-modified SiPc polymers.[11] We note that

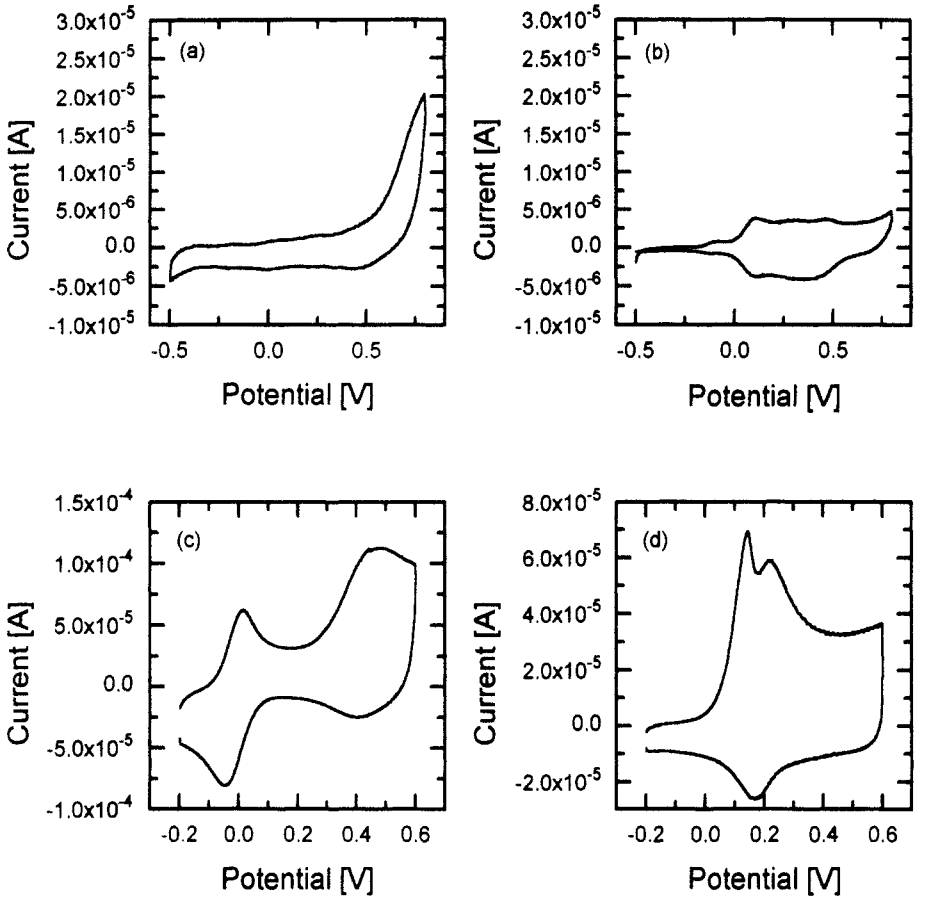

Figure 9. Voltammograms recorded at 5 mV/s for (a) a bare Au electrode, (b) a 3 ML PcPS/Au thin film in 0.1 M HNO_3/(90% H_2O/10% MeOH), (c) the bare Au electrode in contact with the same electrolyte with 10^{-3} M ferrocene, and (d) the 3 ML PcPS/Au in b in contact with the same electrolyte as in c. The first oxidative event observed in d corresponds to the oxidation of the PcPS film, followed by the oxidation of ferrocene, which is displaced from the potential seen on the bare Au electrode.

the onset for oxidation (0.05 V) of the PcPS thin films in CH_3CN is within a few mV of the first oxidation potentials for a soluble form of the cofacially polymerized trimer SiPc (*t*-SiPc 0.08 V) and sparingly soluble forms of the crystalline polymer–SiPc systems, which we examined previously.[15] In those studies it was demonstrated that the oxidation process of the SiPc oligomers was resolvable into multiple one-electron steps, the number observable and their potentials being dependent upon the number of cofacial Pc rings in the oligomer. The monomer SiPc showed the first oxidation positive of the first oxidation potential of the trimer SiPc at ca. 0.6 V. Those data suggested that, in the absence of other factors limiting oxidation, high molecular weight PcPS "hairy-rods" ought to oxidize by one electron at potentials less positive than 0.3 V. We hypothesize that the most easily oxidized PcPS molecules undergo that one-electron oxidation at the least positive potentials in the voltammograms shown in this study, which places their oxidation potentials near the point expected for the free polymer in solution. Voltammetry conducted for the soluble polymer and low molecular weight oligomers do indeed demonstrate oxidation events at near those potentials.[26] Previous voltammetric studies of the trimer SiPc also showed that the second and third one-electron oxidation steps occured at potentials near +0.5 and +0.9 V, respectively, suggesting that it should be possible to fully oxidize each Pc ring in a SiPc oligomer by one electron at potentials less than 1.0 V.

The combination of electrochemical, spectroelectrochemical, ESR, and XPS data collected during the oxidation of these PcPS films suggest that 100% oxidation of each Pc ring by one electron may be achievable at potentials less positive than 1.0 V in nonaqueous solvents. This is approximately half the applied potential apparently needed in previous solution studies of the crystalline forms of SiPc polymers, and for the solubilized versions of these same SiPc polymers to achieve the same apparent level of oxidation.[11] The reasons for this apparent difference in reactivity require additional study but are certainly related to the difficulty in achieving facile electron transfer to crystalline SiPc (for the unmodified SiPc polymers). The origin of the differences in electrochemical behavior between the tetra-*tert*-butyl-modified SiPc polymers and these PcPS films is less clear but may arise from the densification of these PcPS films, where interchain hopping of charge is certainly more facile than for the solution soluble cases and may facilitate oxidation of Pc rings throughout the assembly. More studies are clearly needed for low coverages of such polymeric materials, where the oxidation of isolated PcPS chains can be studied.

Figure 10a shows a reproduction of a TEM micrograph of a PcPS thin film, produced from a slightly lower molecular weight version of PcPS, and transferred after LB deposition to a TEM grid suitable for imaging purposes.[5,6h] Despite the differences in PcPS and film geometries there are several features of this TEM micrograph that are worth considering for the studies presented here and which may be general to most of the PcPS LB film-forming polymers. The individual strands of PcPS are clearly visible, aligned mainly along the dipping direction during LB film formation. The spacing between the chains (12 Å) is consistent with the closest packing expected from these highly ordered arrays, with a space of ca. two C_8 chains separating each Pc ring. Despite the overall quality of these films, there are still several types

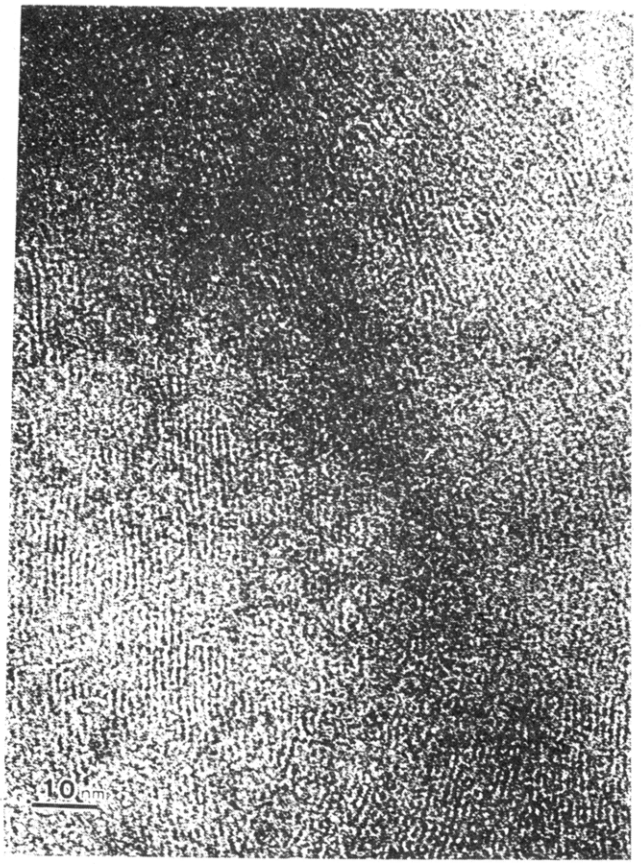

Figure 10. (Top) transmission electron micrograph of a PcPS film supported on a carbon grid. The individual PcPS rods are visible, and a reasonably high degree of ordering is observable, with the rods aligned approximately along the dipping direction taken during the formation of these LB films (reprinted with permission from ref 6k. Copyright 1991 Elsevier). (Bottom) schematic of a cross section of a 5 ML PcPS film showing variable-length PcPS chains, tilted chains, and chain ends as defects and possible penetration sites for a counterion such as ClO_4^- during the oxidation process.

of defects which can be identified and which probably contribute to the electrochemical properties of these films. There are clear regions where long strands of PcPS intersect at angles of between 5 and 30°, causing interruptions to the ordering which can extend up to 5–20 nm. There also appear to be pockets where few long PcPS chains are visible and where the average length of PcPS chain appears to be 10–15 Pc units. Whether these domains arise as a result of preparing the LB films for TEM characterization is not clear, but it is reasonable to assume that they exist to some extent in the electrochemically characterized materials. The overall organization of these thin films is consistent with previous studies of "hairy rod" polymers which show film structures which mimic the flow profiles of these polymers as they organize on the LB trough during the actual transfer to solid substrates.[6h] It is important to realize that at the termination of each of the PcPS chains we also expect silanol groups or products of reactions of those silanol groups which leave ionizable –OH or halide end groups at sites of disorder in these films.[6a–e]

Figure 10b shows a schematic view of a cross section of a PcPS LB film, with multiple layers of PcPS represented, the likelyhood of variable chain lengths and PcPS orientations coexisting in a multilayer stack of these rigid polymers. The chain ends have been intentionally unlabeled but are presumed to be sites of higher dielectric strength and, therefore, likely to be the points of entry of counterions of both charges. The question of the extent of solvent penetration, especially for oxidation in aqueous environments, is not answerable at the present time. From the demonstrated stability of the oxidized forms of these PcPS films, however, we anticipate relatively little penetration of H_2O into the PcPS film during electrolysis, which would lead to decomposition of the cation radical products. The packing density of these PcPS films appears to preclude much solvent penetration and may therefore be the principle reason for the low D_{app} values determined in our spectroelectrochemical experiments. About 25% of an unannealed PcPS film, when undergoing oxidation in contact with H_2O, is clearly capable of facile electron and counterion transport and rapid equilibration with the substrate electrode. The remaining PcPS, oxidizing up to 80–100% of the available Pc rings, whether in contact with H_2O or CH_3CN, does not readily reach electrochemical equilibrium with the substrate electrode. Further experiments are needed to determine whether this lack of equilibration is due to limitations of electron transport between PcPS strands, counterion transport, and/or solvent permeation. There are also strong effects of the cross-linking of these PcPS chains on their electrochemical properties, which undoubtedly arise from similar non-equilibrium processes. Such effects will have some bearing on the use of PcPS and related polymers as patternable and electrochemically addressable supromolecular assemblies.

Acknowledgment. Support for this research effort was provided by Fonds der Chemischen Industrie (A.F.), the Max Planck Institute für Polymerforschung, the Alexander von Humboldt Stiftung (N.R.A.), and the National Science Foundation (N.R.A.). The authors gratefully acknowledge the efforts of Ken Nebesny and Paul Lee of the University of Arizona for help in acquiring the XPS data and of Jürgen Saalmüller at the MPIP for assistance in the ESR experiments, the gift of the spectroelectrochemical cell from Bruce Henne at Kodak, and helpful discussions from Stefan Schwiegk of the MPIP.

References and Notes

(1) (a) Surridge, N. A.; Jernigan, J. C.; Dalton, E. F.; Buck, R. P.; Watanabe, M.; Zhang, H.; Pinkerton, M.; Wooster, T. T.; Longmire, M. L.; Facci, J. S.; Murray, R. S. *Faraday Discuss. Chem. Soc.* **1989**, *88*, 1 and references cited therein. (b) Murray, R. W. *Annu. Rev. Mater. Sci.* **1984**, *14*, 145. (c) White, B. A.; Murray, R. W. *J. Am. Chem. Soc.* **1987**, *109*, 2576. (d) Jernigan, J. C.; Murray, R. W. *J. Am. Chem. Soc.* **1990**, *112*, 1034. (e) Pinkerton, M. J.; Mest, Y. L.; Zhang, H.; Watanabe, M.; Murray, R. W. *J. Am. Chem. Soc.* **1990**, *112*, 3730. (f) Zhang, H.; Murray, R. W. *J. Am. Chem. Soc.* **1991**, *113*, 5183.

(2) (a) Daum, P.; Lenhard, J. R.; Rolison, D.; Murray, R. W. *J. Am. Chem. Soc.* **1980**, *102*, 4649. (b) Majda, M.; Faulkner, L. *J. Electroanal. Chem.* **1984**, *222*, 223. (c) Buck, R. P. *J. Electroanal. Chem.* **1988**, *243*, 279; *J. Phys. Chem.* **1988**, *92*, 4196.

(3) (a) Nowak, M. J.; Spiegel, D.; Hotta, S.; Heeger, A. J.; Pincus, P. A. *Macromolecules* **1989**, *22*, 2917. (b) Patil, A. O.; Heeger, A. J.; Wudl, F. *Chem. Rev.* **1988**, *88*, 183. (c) Ofer, D.; Crooks, R. M.; Wrighton, M. S. *J. Am. Chem. Soc.* **1990**, *112*, 7869. (d) Guay, J.; Diaz, A.; Wu, R.; Tour, J. M. *J. Am. Chem. Soc.* **1993**, *115*, 1869.

(4) (a) Hillman, A. R.; Swann, M. J.; Bruckenstein, S. *J. Phys. Chem.* **1991**, *95*, 3271. (b) Bruckenstein, S.; Hillman, A. R. *J. Phys. Chem.* **1991**, *95*, 10748.

(5) Wegner, G. *Mol. Cryst. Liq. Cryst.* **1993**, *235*, 1.

(6) (a) Sauer, T.; Arndt, T.; Batchelder, D. N.; Kalachev, A. A.; Wegner, G. *Thin Solid Films* **1990**, *187*, 357. (b) Sauer, T.; Caseri, W.; Wegner, G.; Vogel, A.; Hoffman, B. *J. Phys. D. Appl. Phys.* **1990**, *23*, 79. (c) Embs, F.; Funhoff, D.; Laschewsky, A.; Licht, U.; Ohst, H.; Prass, W.; Ringsdorf, H.; Wegner, G.; Wehrmann, R. *Adv. Mater.* **1991**, *3*, 25. (d) Wegner, G.; Rühe, J. *Faraday Discuss. Chem. Soc.* **1989**, *88*, 333. (e) Kaltbeitzel, A.; Neher, D.; Bubeck, C.; Sauer, T.; Wegner, G.; Caseri, W. Electronic Properties of Conjugated Polymers. Kuzmany, H., Mehring, M., Roth, S., Eds. *Springer Ser. Solid State Sci.* **1989**, *91*, 220. (f) Neher, D.; Kaltbeitzel, A.; Wolf, A.; Bubeck, C.; Wegner, G. In *Cojugated Polymeric Materials: Opportunities in Electronics, Optoelectronics, and Molecular Materials*; Bredas, J. L., Chance, R. R., Eds.; Kluwer Academic Publishers: New York, 1990; p 387. (g) Schwiegk, S.; Vahlenkamp, T.; Xu, Y.; Wegner, G. *Macromolecules* **1992**, *25*, 2513. (h) Schwiegk, S.; Fischer, H.; Xu, Y.; Kremer, F.; Wegner, G. *Makromal. Chem. Macromal. Symp.* **1991**, *46*, 211. (i) Schaub, M.; Mattamer, K.; Schwiegk, S.; Albouy, P.-A.; Wenz, G.; Wegner, G. *Thin Solid Films* **1992**, *210*, 397. (j) Schwiegk, S.; Werth, M.; Leisen, J.; Wegner, G.; Speiss, H. *Acta Polymer* **1993**, *44*, 31. (k) Yase, K.; Schwiegk, S.; Lieser, G.; Wegner, G. *Thin Solid Films* **1992**, *211*, 22; **1992**, *213*, 130.

(7) Watanabe, I.; Hong, K.; Rubner, M. F. *Langmuir* **1990**, *6*, 1164.

(8) Fujiki, M.; Tabei, H.; Kurihara, T. *J. Phys. Chem.* **1988**, *92*, 1281.

(9) (a) Hua, Y. L.; Roberts, G. G.; Ahmad, M. M.; Petty, M. C. *Philosoph. Mag. B* **1986**, *53*, 105. (b) Lever, A. B. P.; Licoccia, S.; Magnell, K.; Minor, P. C.; Ramaswamy, B. S. *Am. Chem. Soc. Symp. Ser.* **1982**, *201*, 237.

(10) (a) Chidsey, C. E. D. *Science* **1991**, *251*, 919. (b) Liu, M. D.; Leidner, C. R.; FAcci, J. S. *J. Phys. Chem.* **1992**, *96*, 2804. (c) Facci, J. S.; Falcigno, P. A.; Gold, J. M. *Langmuir* **1986**, *2*, 732. (d) Facci, J. S. *Langmuir* **1987**, *3*, 525. (e) Obeng, Y. S.; Bard, A. J. *Langmuir* **1991**, *7*, 195.

(11) (a) Gaudiello, J. G.; Kellog, G. E.; Tetrick, S. M.; Marks, T. J. *J. Am. Chem. Soc.* **1989**, *111*, 5259. (b) Almeida, M.; Gaudiello, J. G.; Kellog, G. E.; Tetrick, S. M.; Marcy, H. O.; McCarthy, W. J.; Butler, J. C.; Kannewurf, C. R.; Marks, T. J. *J. Am. Chem. Soc.* **1989**, *111*, 5271. (c) Marks, T. J. *Science* **1985**, *227*, 881 and references cited therein. (d) Dirk, C. W.; Inabe, T.; Schoch, K. F.; Marks, T. J. *J. Am. Chem. Soc.* **1983**, *105*, 1539. (e) Diel, B. N.; Inabe, T.; Lyding, J. W.; Schoch, K. F., Jr.; Kannewurf, C. R.; Marks, T. J. *J. Am. Chem. Soc.* **1983**, *105*, 1551. (f) Gale, D. C.; Gaudiello, J. G. *J. Am. Chem. Soc.* **1991**, *113*, 1610.

(12) (a) Snow, A. W.; Barger, W. R.; Klusty, M.; Wohltjen, H.; Jarves, N. L. *Langmuir* **1986**, *2*, 260. (b) Fujiki, M.; Tabei, H. *Langmuir* **1988**, *4*, 320. (c) Burack, J. J.; LeGrange, J. D.; Markham, J. L.; Rockward, W. *Langmuir* **1992**, *8*, 613. (d) Ogawa, K.; Kinoshita, S.-I.; Yonehara, H.; Nakahara, H.; Fukada, K. *J. Chem. Soc., Chem. Commun.* **1989**, 477. (e) Shutt, J. D.; Batzel, D. A.; Sudiwala, R. V.; Rickert, S. E.; Kenney, M. E. *Langmuir* **1988**, *4*, 1240.

(13) (a) Wynne, K. J. *Inorg. Chem.* **1985**, *24*, 1339. (b) Nohr, R. S.; Kuznesof, P. M.; Wynne, K. J.; Kenney, M. E.; Siebenman, P. G. *J. Am. Chem. Soc.* **1981**, *103*, 4371. (c) Collman, J. P.; McDevitt, J. T.; Leidner, C. R.; Yee, G. T.; Torrance, J. B.; Little, W. A. *J. Am. Chem. Soc.* **1987**, *109*, 4606. (d) Futamata, M. *Mol. Cryst. Liq. Cryst.* **1991**, *197*, 109.

(14) (a) Cieslinski, R.; Armstrong, N. R. *Anal. Chem.* **1979**, *51*, 565. (b) White, J. R.; Armstrong, N. R. *J. Electroanal. Chem.* **1982**, *131*, 121.

(15) (a) Mezza, T. M.; Armstrong, N. R.; Kenney, M. E. *J. Electroanal. Chem.* **1981**, *124*, 311. (b) Mezza, T. M.; Armstrong, N. R.; Kenney, M. E. *J. Electroanal. Chem.* **1984**, *176*, 259. (c) Mezza, T. M. PhD Dissertation, University of Arizona, 1982. (d) Wheeler, B. L.; Nagasubramanian, G.; Bard, A. J.; Schechtman, L. A.; Dininny, d. R.; Kenney, M. E. *J. Am. Chem. Soc.* **1984**, *106*, 7404.

(16) (a) Nebesny, K. W.; Maschhoff, B. L.; Armstrong, N. R. *Anal. Chem.* **1989**, *61*, 469A. (b) Seah, M. P. In Practical Surface Analysis by Auger and X-ray Photoelectron Spectroscopy; Briggs, D., Seah, M. P., Eds.; John Wiley and Sons: New York, 1983; pp 181–216.

(17) Goedel, W.; Hölz, G.; Wegner, G.; Rosenmund, J.; Zotti, G. *Polymer (London)*, submitted.

(18) (a) Armstrong, N. R.; Nebesny, K. W.; Collins, G. E.; Chau, L.-K.; Lee, P. A.; England, C.; Diehl, D.; Douskey, M.; Parkinson, B. A. Science and Technology of Thin Films for the 21st Century. Chang, R. P. H., Ed. In *Thin Solid Films* **1992**, *216*, 90. (b) Collins, G. E.; Nebesny, K. W.; England, C. D.; Chau, L.-K.; Lee, P. A.; Parkinson, B. A.; Armstrong, N. R. *J. Vac. Sci. Technol.* **1992**, *10(4)*, 2902. (c) Chau, L.-K.; Arbour, C.; Collins, G. E.; Nebesny, K. W.; Lee, P. A.; England, C. D.; Armstrong, N. R.; Parkinson, B. A. *J. Phys. Chem.* **1993**, *97*, 2690. (d) Chau, L.-K.; England, C. D.; Chen, S.-Y.; Armstrong, N. R. *J. Phys. Chem.* **1993**, *97*, 2699.

(19) (a) Yanagi, H.; Douko, S.; Ueda, Y.; Ashida, M.; Wörhle, D. *J. Phys. Chem.* **1992**, *96*, 1366. (b) Dann, A. J.; Hoshi, H.; Maruyama, Y. *J. Appl. Phys.* **1990**, *66*, 1371 and 1845.

(20) (a) Kasha, M. In *Spectroscopy of the Excited State*; DiBartole, B., Ed.; Plenum Press: New York, 1976. (b) Hochstrasser, R. M.; Kasha, M. *Photochem. Photobiol.* **1964**, *3*, 317. (c) Czikkely, V.; Försterling, H. D.; Kuhn, H. *Chem. Phys. Lett.* **1970**, *6*, 11. (d) Büchner, H.; Kuhn, H. *Chem. Phys. Lett.* **1970**, *6*, 183.

(21) Genies, E. M.; Pernaut, J. M. *Synth. Metals* **1984**, *10*, 117.

(22) (a) Tanguy, J.; Mermilliod, N.; Hoclet, M. *J. Electrochem. Soc.* **1987**, *134*, 795. (b) Zhou, Q.-X.; Kolaskie, C. J.; Miller, L. L. *J. Electroanal. Chem.* **1987**, *223*, 283. (c) Yeu, T.; Ngyuen, T. V.; White, R. E. *J. Electrochem. Soc.* **1988**, *135*, 1971. (d) Hsu, D.-F.; Gratzl, M.; Riley, A. M.; Janata, J. *J. Phys. Chem.* **1990**, *94*, 5982.

(23) (a) Feldberg, S. W. *J. Am. Chem. Soc.* **1984**, *106*, 4671. (b) Feldberg, S. W.; Rubenstein, I. *J. Electroanal. Chem.* **1988**, *240*, 1.

(24) (a) Briggs, D. In *Practical Surface Analysis by Auger and X-ray Photoelectron Spectroscopy*; Briggs, D., Seah, M. P., Eds.; John Wiley and Sons: New York, 1983; pp 359–396. (b) Schmidt, J. J.; Gardella, J. A., Jr.; Salvati, L., Jr. *Macromolecules* **1989**, *22*, 4489.

(25) (a) Hush, N. S.; Woolsey, I. S. *Molec. Phys.* **1971**, *21*, 465. (b) Hush, N. S.; Cheung, A. S. *Chem. Phys. Lett.* **1977**, *47*, 1.

(26) Schlettwein, D.; Ferencz, A.; Lee, P. A.; Nebesny, K. W.; Wegner, G.; Armstrong, N. R., manuscript in preparation.